Supporting Information

A Low-Power White Light Triggered AIE Polymer Nanoparticles with High ROS Quantum Yield for Mitochondria-Targeted and Image-Guided Photodynamic Therapy †

Yadan Zheng[a], Hongguang Lu*[a], Zhu Jiang[a], Yue Guan[a], Jialing Zou[a], Xian Wang[a], Ruoyu Cheng[a], Hui Gao*[a]

[a]School of Chemistry and Chemical Engineering, Tianjin Key Laboratory of Organic Solar Cells and Photochemical Conversion, Tianjin University of Technology, Tianjin 300384, P. R. China. E-mail: hglu@tjut.edu.cn; hgao@tjut.edu.cn.

† Electronic Supplementary Information (ESI) available. See DOI: 10.1039/b000000x/

Contents

1. Experimental section

1.1 General information

All chemicals and solvents were commercially available and were used without further purification. Rose Bengal, methacryloyl chloride, bis(dibenzylideneacetone)palladium(0) [$Pd_2(dba)_3$], 2-dicyclohexylphosphino-2',6'-diisopropoxybiphenyl (Ruphos) were purchased from Aladdin (Tianjin, China). 3,5-Bis(trifluoromethyl)phenylacetonitrile, 4-hydroxydiphenylamine, 1,4-dibromo-2,5-dimethylbenzene, tripheylphosphine, dichlorofluorescein diacetate (DCF-DA), bis(2-bromoethyl) ether were purchased from Heowns (Tianjin, China). 2,5-Dibromoterephthalaldehyde, *N*-pheny-4-(tetrahydro-2*H*-pyran-2-yi)oxy)aniline, (2*Z*,2'*Z*)-3,3'-(2,5-dibromo-1,4-phenylene) bis(2-(3,5-bis(trifluoromethyl)phenyl)acrylonitrile) and *N*-(2-hydroxypropyl) methacrylamide (HPMA) were synthesized according to the literature,[1-4] respectively. 9,10-Anthracenediyl-bis(methylene)dimalonic acid (ABDA), fetal bovine serum (FBS) and RPMI 1640 culture medium were commercially available from Sigma-Aldrich. 3-(4,5-Dimethyl thiazol-2-yl)-2,5-diphenyltetrazolium bromide (MTT) was used in the cell cytotoxicity assay (Dojindo, Japan). A549 cells and HeLa cells were obtained from Life Technologies (Carlsbad, CA).

^{1}H NMR spectra were recorded with a Bruker AV-400 (400 MHz) spectrometer at room temperature with tetramethylsilane (TMS, δ = 0 ppm) as an internal standard. ^{13}C NMR spectra were determined on a Bruker AV-400 (100 MHz) spectrometer with tetramethylsilane (TMS, δ = 0 ppm) as an internal standard. HRMS was performed on a Waters Xevo Q-TOF MS with an ESI source. Waters 2414 GPC was used for polymer molecular weight determination. UV-vis spectra were recorded on a Shimadzu UV-3390 spectrophotometer. Fluorescence spectra were carried out with a Hitachi F4500 spectrofluorophotometer. Dynamic light scattering (DLS) measurements were performed using a Malvern Nano-ZS instrument at room temperature. The morphology of nanoparticles (NPs) was observed using a JEOL JSM-6700F type field emission scanning electron microscope (SEM).

The geometries of T1 and S1 state were optimized by B3LYP and TD-B3LYP method, respectively. Then the energy of T1 state and S1 state at their equilibrium geometries were

evaluated by TD-B3LYP method, the energy difference corresponds to adiabatic singlet-triplet energy splitting. Gaussian 09 package (Revision D.01) and 6-31G* basis set were used in all the calculations.[5, 6]

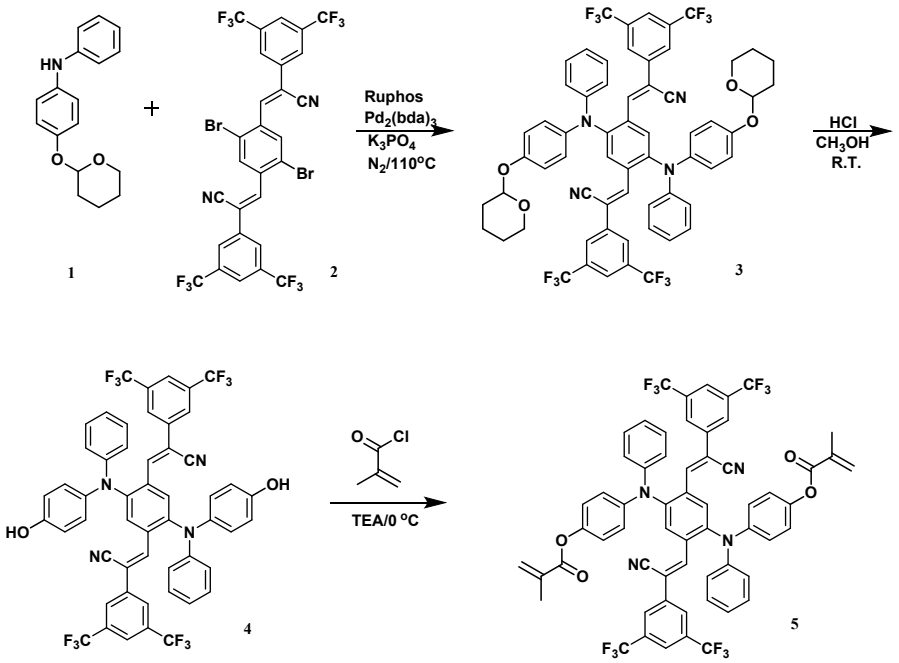

Scheme S1. Synthetic route to AIEM.

1.2 Synthesis of monomers and polymers

Synthesis of (2*Z*,2'*Z*)-3,3'-(2,5-bis(phenyl(4-((tetrahydro-2*H*-pyran-2-yl)oxy)phenyl) amino)-1,4-phenylene)bis(2-(3,5-bis(trifluoromethyl)phenyl)acrylo nitrile) (3)

A flask was charged with **1** (5.0 mmol, 1.347 g), **2** (0.5 mmol, 0.381 g), $Pd_2(dba)_3$ (0.038 mmol, 0.035 g), Ruphos (0.15 mmol, 0.070 g), K_3PO_4 (5.0 mmol, 1.061 g) and toluene (2 mL). The mixture was then degassed, purged with N_2 and heated at 110 °C for 24 h. The reaction mixture was cooled to room temperature, followed by addition of water (30 mL) and chloroform (50 mL). An organic layer was separated and washed with brine, dried over anhydrous magnesium sulfate and evaporated to dryness under reduced pressure. The crude product was purified by recrystallization from $CHCl_3$/ethanol to give **3**. Yield: 64%, a dark red solid. ^{1}H NMR (400 MHz, DSMO-d_6, TMS, ppm): δ 8.12–8.14 (d, J = 8.4 Hz, 4H), 7.88 (s, 4H), 7.59 (s, 2H), 7.22–7.26 (t, J = 8.0 Hz, 4H), 7.05–7.07 (d, J = 8.8 Hz, 4H), 6.99–7.01 (d, J = 8.0 Hz, 4H), 6.90–6.93 (m, 6H), 5.22–5.23 (t, J = 6.4 Hz, 2H), 3.59–3.64 (m, 2H), 3.31–3.43 (m, 2H), 1.47–1.88 (m, 12H); ^{13}C NMR (100 MHz, $CDCl_3$, TMS, ppm): δ 153.82,

148.11, 143.48, 142.70, 141.45, 136.49, 133.60, 132.52, 132.18, 131.85, 131.77, 129.72, 127.83, 126.07, 125.75, 124.20, 122.73, 122.28, 121.48, 117.91, 115.80, 111.52, 96.75, 62.06, 30.31, 25.15, 18.79; HRMS (ESI): *m/z*: Calcd for $C_{62}H_{47}F_{12}N_4O_4$: 1139.3400; $[M+H]^+$: Found: 1139.3388.

Synthesis of (2*Z*,2'*Z*)-3,3'-(2,5-bis((4-hydroxyphenyl)(phenyl)amino)-1,4-phenylene) bis(2-(3,5-bis(trifluoromethyl)phenyl)acrylonitrile) (4)

Compound **3** (3.0 mmol, 3.417g) was dissolved into 100 mL of THF and 5 mL of methanol, and then 10 mL of 2N HCl aqueous solution was added into the solution. The reaction mixture was stirred at room temperature for 12 h. After the solvent was removed under reduced pressure, the residue was purified by silica gel chromatography (light petroleum/ethyl acetate = 5/1) to yield **4**. Yield: 89%, a rose red solid. ^{1}H NMR (400 MHz, DMSO-d_6, TMS, ppm): δ 9.32 (s, 2H), 8.13 (s, 4H), 7.85 (s, 4H), 7.57 (s, 2H), 7.18–7.22 (t, *J* = 8.0 Hz, 4H), 6.98–7.00 (d, *J* = 8.0 Hz, 4H), 6.91–6.93 (d, *J* = 8.0 Hz, 4H), 6.83–6.86 (m, 2H), 6.65–6.67 (d, *J* = 8.4 Hz, 4H); ^{13}C NMR (100 MHz, DMSO-d_6, TMS, ppm): δ 154.65, 148.62, 145.40, 143.09, 143.30, 149.11, 136.27, 132.65, 131.77, 131.44, 131.11, 130.78, 129.72, 127.80, 127.03, 124.77, 123.07, 122.05, 121.79, 121.23, 116.66, 116.46, 116.17, 114.72, 111.33; HRMS (ESI): *m/z*: Calcd for $C_{52}H_{31}F_{12}N_4O_2$: 971.2250; $[M+H]^+$: Found: 971.2238.

Synthesis of (2*Z*,2'*Z*)-3,3'-(2,5-bis((4-methylacrylate)(phenyl)amino)-1,4-phenylene) bis(2-(3,5-bis(trifluoromethyl)phenyl)acrylonitrile) (5)

A flask was charged with a solution of **4** (7.2 mmol, 7.0 g) and triethylamine (21.6 mmol, 2.181 g) in 300 mL THF, then a THF solution (10 mL) of methacryloyl chloride (21.6 mmol, 2.258 g) was added dropwise within 30 min at 0°C. The reaction mixture was stirred at room temperature overnight. Then, the reaction mixture was filtered to remove a generated precipitate. After the solvent was removed under reduced pressure, the residue was purified by silica gel chromatography (light petroleum/ethyl acetate= 10/1) to yield **5** as red solid. Yield: 78%, a red solid. ^{1}H NMR (400 MHz, DMSO-d_6, TMS, ppm): *δ* 8.15 (s, 2H), 8.11 (s, 2H), 7.88 (s, 4H), 7.64 (s, 2H), 7.25–7.29 (t, *J* = 8.0 Hz, 4H), 7.09–7.12 (m, 8H), 7.04–7.06

(d, J = 8.8 Hz, 4H), 6.95–6.99 (m, 2H), 6.21 (s, 2H), 5.86 (s, 2H), 1.96 (s, 6H); ^{13}C NMR (100 MHz, $CDCl_3$, TMS, ppm): δ 165.76, 147.44, 146.77, 144.98, 143.31, 142.39, 135.82, 135.74, 132.88, 132.55, 132.16, 131.87, 129.96, 128.35, 127.30, 126.15, 124.39, 124.18, 123.65, 123.20, 123.01, 121.47, 115.72, 112.40, 18.31; HRMS (ESI): *m/z*: Calcd for $C_{60}F_{12}H_{38}N_4O_4Na$: 1129.2594; $[M+Na]^+$: Found: 1129.2641.

Synthesis of (2-(2-bromoethoxy)ethyl)triphenylphosphonium (6)

Bis(2-bromoethyl)ether (5.0 mmol, 1.16 g) and tripheylphosphine (10.0 mmol, 2.62 g) were dissolved in acetonitrile (50 mL), and the mixture was stirred under reflux for 12 h. Then, the mixture was cooled to room temperature. The solvent was then removed by evaporation under pressure, and the residue was recrystallized from a mixture of dichloromethane/ethyl acetate to yield **6** as a white solid. ^{1}H NMR (400 MHz, DMSO-d_6, TMS, ppm) δ 7.92–7.78 (m, 15H), 3.60–3.63 (t, J = 6.4 Hz, 2H), 3.41–3.45 (m, 4H), 1.97–2.04 (m, 2H).

Synthesis of HPMA-TPP

HPMA (1.0 mmol, 0.143 g) and compound 6 (1.0 mmol, 0.414 g) was dissolved in dichloromethane (5 mL). NaH was added to the reaction mixture at 0°C. The reaction mixture was stirred at room temperature overnight. Then, the reaction mixture was filtered to remove a generated precipitate. The ethyl acetate was added into the solvent to precipitate the white solid for further step.

Synthesis of polymers

HPMA (0.105 mmol 15.0 mg), HPMA-TPP (0.245 mmol, 117.0 mg), AIEM (0.025 mmol, 28.0 mg), 2-aminoethyl methacrylate (0.0035 mmol, 2.0 mg), and AIBN (0.0122 mmol, 2.0 mg) were dissolved in DMF (1 mL). The solution was degassed three times through a standard freeze-thaw process. The monomers were polymerized at 65^{o}C for 24 h under N_2. And then the mixture was dialyzed against Milli-Q water for 20 h and ethanol for 4 h using 3500 Da M_w cutoff dialysis membranes. Finally, the solution in dialysis bag was carried out by evaporation under pressure to obtain the polymer PAIE-TPP. ^{1}H NMR (400 MHz, DMSO-d_6, TMS, ppm) δ 8.12-7.03 (broad, aromatic protons, 7.68-7.86 from the TPP

unit), 4.71 (broad, -OH), 3.67 (broad, -CH_3CHOH-), 2.91 (broad, -CH_2NH-), 1.24 (broad, -CH_2-), 0.86-1.00 (broad, -CH_3). M_n = 13100, M_w = 17200, M_w/M_n = 1.31. As the control test, polymer PAIE was synthesized using similar methods as that of PAIE-TPP, except that no TPP was added. ^{1}H NMR (400 MHz, DMSO-d_6, TMS, ppm) δ 8.12-7.03 (broad, aromatic protons), 4.71 (broad, -OH), 3.67 (broad, -CH_3CHOH-), 2.91 (broad, -CH_2NH-), 1.24 (broad, -CH_2-), 0.86-1.00 (broad, -CH_3). M_n = 11300, M_w = 15800, M_w/M_n = 1.40.

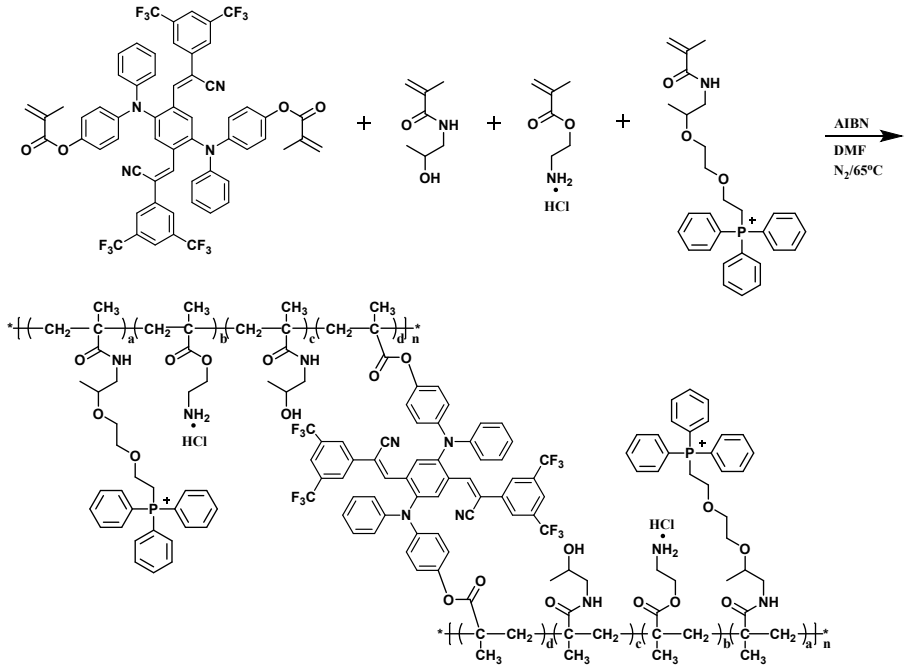

Scheme S2. Synthetic of AIEM conjugated polymer PAIE-TPP.

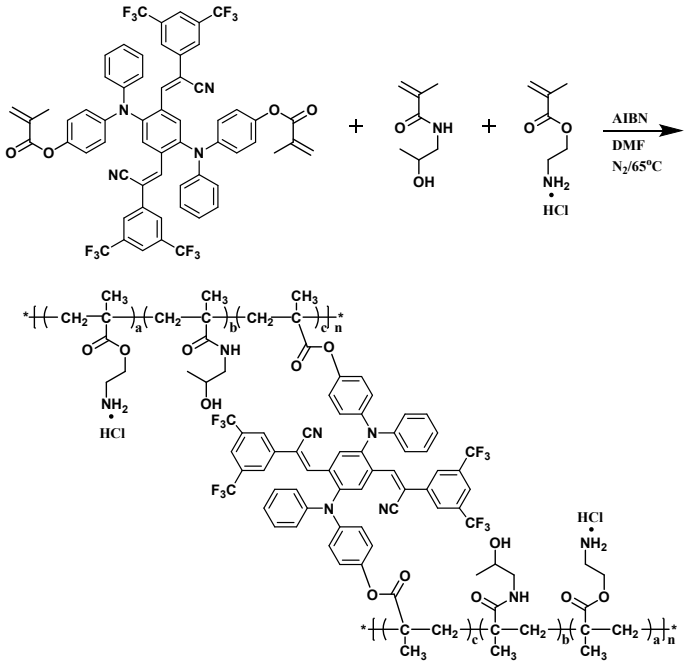

Scheme S3. Synthetic of AIEM conjugated polymer PAIE.

1.3 Preparation of PAIE-TPP NPs

PAIE-TPP (10mg) was dissolved in 1mL of DMSO to make a stock liquid (10 mg mL^{-1}). 20 μL of the stock liquid was added in 980 μL Milli-Q water slowly. The DMSO/water mixture was sonicated for 2 min and filtered through 0.45 μm microfilter to collect the PAIE-TPP NPs suspension. PAIE NPs were also prepared following the same procedure.

1.4 Detection of ROS generation from the AIE NPs in solution

To study the ability to generate ROS of the AIEM NPs and PAIE-TPP NPs, dichlorofluorescein diacetate (DCF-DA) was used to detect the ROS generation upon light irradiation. To convert DCF-DA to dichlorofluorescein, 0.25 mL of 1 mM DCF-DA in ethanol was added to 1 mL of 0.01N NaOH and allowed to stir for half an hour at room temperature. The hydrolysate was then neutralized with 5 mL of 1× PBS at pH 7.4, and stored in ice until further use. 10 μL of the above solution was mixed with 1 mL of AIEM (25μM) or PAIE-TPP NPs (200 μg mL^{-1}) and exposed to white light irradiation for different time intervals at a power density of 4 mW cm^{-2}. The fluorescence change in the solution was measured with excitation at 488 nm and the emission was collected at 525 nm.

1.5 ROS quantum yield measurements.

The ROS quantum yield of AIE NPs in water (Φ) upon white light irradiation (400-800 nm, 4 mW cm^{-2}) was determined using 9,10-anthracenediyl-bis(methylene) dimalonic acid (ABDA) as an indicator and using Rose Bengal (RB) as the standard reference. ABDA solid (200 μM) was dissolved in DI water. The PAIE-TPP NPs (200 μg mL^{-1}) or RB (5 μg mL^{-1}) was then added in aqueous solution. The absorbance decrease of ABDA at 400 nm was recorded for different durations of light irradiation to obtain the decay rate of the photosensitizing process. And the ROS yield is calculated using the following equation:

$$\Phi_{\text{PAIE-TPP}} = \Phi_{\text{RB}} (K_{\text{PAIE-TPP}} \cdot A_{\text{RB}}) / K_{\text{RB}} \cdot A_{\text{PAIE-TPP}}$$

Where $K_{\text{PAIE-TPP}}$ and K_{RB} are the decomposition rate constants of the photosensitizing process determined by the plot ln (A_0/A) versus irradiation time. A_0 is the initial absorbance of ABDA while A is the ABDA absorbance after different irradiation times. $A_{\text{PAIE-TPP}}$ and A_{RB} represent the light absorbed by AIE NPs and RB, which are determined by integration of the

absorption bands in the wavelength range of 400-800 nm. Φ_{RB} is the ROS quantum yield of RB, which is 0.75 in water. The decomposition rate constants of PAIE-TPP NPs ($K_{PAIE\text{-}TPP}$) and RB (K_{RB}) were calculated as 0.00104 and 0.00051, respectively (Figure 1E and Figure S6). The integrations of the optical absorption in the wavelength range of 400-800 nm for RB (A_{RB}) and PAIE-TPP ($A_{PAIE\text{-}TPP}$) were 18.153 and 35.182, respectively.

1.6 Cell culture and imaging

Both cells were cultured in culture medium (RPMI 1640) containing 10% FBS, 1% penicillin streptomycin, and incubated at 37 °C in a 5% CO_2 atmosphere. Cells were seeded onto 35 mm glass-bottom dishes and allowed to grow until a confluence of 80%. Prior to experiments, the medium was removed and the adherent cells were washed twice with PBS buffer to remove the remnant growth medium.

The PAIE-TPP NPs and PAIE NPs stock liquid (10 mg mL^{-1}) were then added to the cell plates with final concentration in culture medium of 40 μg mL^{-1} and incubation for 3 h. The stained cells were then washed three times with PBS buffer. And the mitochondria were stained with Mito-Tracker Green (50 nM) for 15 minutes, which were further washed three times with PBS buffer and used for bioimaging subsequently. Under a Nikon A1 confocal laser microscope system (CLMS), PAIE-TPP NPs and PAIE NPs was excited at 488 nm and the emission was collected at range of 662-737 nm. Mito-Tracker Green was excited at 488 nm and the emission was collected at range of 500-530 nm. No background fluorescence of cells was detected under the setting condition.

1.7 Flow cytometric analysis

To demonstrate the cellular uptake of AIE NPs (PAIE-TPP or PAIE), fluorescence measurements (λ_{ex} = 488 nm, λ_{em} = 685-735 nm) were carried out by using a BD LSRFortessa cytometer (Becton, Dickinson and Company, Franklin Lakes, USA). The AIE NPs stock liquid were then added to the cell plates with final concentration in culture medium of 40 μg mL^{-1} and incubation for 3 h. After incubation, the cells were centrifuged, washed twice with fresh medium, and then suspended in fresh medium again. Fluorescence was determined by counting 10,000 events.

1.8 Intracellular ROS detection

ROS generation inside cells under light irradiation was detected using DCF-DA as an indicator. A549 cells were cultured in the plates at 37 ^{o}C. After 80% confluence, the culture medium was removed and washed twice with PBS buffer. Following incubation with AIE NPs (40 μg mL^{-1}) for 3 h in the dark, DCF-DA was loaded into the cells. After 15-min incubation, cells were washed twice with PBS and then exposed to white light for different irradiation time (4 mW cm^{-2}). In parallel experiments, Vitamin C (50 mM) was added as a scavenger of ROS. The medium was replaced with PBS and then upon light irradiation for different time. The fluorescence images of treated cells were acquired using CLMS. The DCF-DA was excited at 488 nm and the emission was collected at 525 nm. No background fluorescence of cells was detected under the setting condition.

1.9 Cytotoxicity study

To determine the cytotoxicity, a MTT-based cell viability test was performed in 96-well plates. A549 cells and HeLa cells were seeded at a density of 5000 cells per well respectively. After overnight culturing, the cells were treated with PAIE-TPP NPs in DMEM suspension at various concentrations for 3 h. PAIE-TPP NPs suspension was then replaced by fresh cell culture medium. The selected wells were exposed to light irradiation (10 mW cm^{-2}, 30 min per 12 h) and further cultured for 48 h. In the parallel experiment, both cell lines were treated with PAIE-TPP NPs for 48 h in the dark. Then, the medium in the wells were removed and the cells were washed with PBS buffer and then incubated in fresh medium (100 μL) and 10 μL of MTT solution (5 mg mL^{-1}) for 3 h. After removing MTT solution, 100 μL of filtered DMSO was added into each well to dissolve all the crystals formed. The cell viability was accessed by means of MTT absorbance at 570 nm recorded using a microplate reader (Epoch, BioTek, Gene company Limited). The cell viability in each well was calculated from the obtained values as a percentage of control wells. The results were presented as a mean and standard deviation obtained from eight samples.

2. Table S1 Comparison of lately reported AIE photosensitizers for PDT.

Photosensitizer	Light source	Light power-density	ROS quantum yield	References
TPE-IQ	UV irradiation	−	−	*Chem. Commun.*, **2014**, *50*, 14451-14454
TPE-red-2A2H	Xenon lamp (500 W) with a filter passing light of 450 nm	12 mW cm^{-2}	−	*Anal. Chem.*, **2014**, *86*, 7987-7995
TPECM-2GFLGD3-cRGD	White light irradiation	250 mW cm^{-2}	−	*Angew. Chem. Int. Ed.*, **2015**, *54*, 1780-1786
TPETP-SS-DEVD-TPS-cRGD	White light irradiation	100 mW cm^{-2}	0.68	*Adv. Funct. Mater.*, **2015**, *25*, 6586-6595
TPECM-TPP	White light irradiation	100 mW cm^{-2}	−	*Chem. Sci.*, **2015**, *6*, 4580-4586
TAT–PPDC NPs	White light irradiation	100 mW cm^{-2}	0.89	*Chem. Sci.*, **2015**, *6*, 5824-5830
TPECB-Pt-D5-cRGD	−	250 mW cm^{-2}	−	*Chem. Commun.,* **2015**, *51*, 8626-8629
FA–AIE–TPP dots	White light irradiation	250 mW cm^{-2}	−	*Adv. Healthcare Mater.*, **2015**, *4*, 2667-2676
TPETSAl	White light irradiation	100 mW cm^{-2}	0.43	*Angew. Chem. Int. Ed.*, **2016**, *55*, 6457-6461
TPETP-AA-Rho-cRGD	−	100 mW cm^{-2}	0.68	*Chem. Sci.*, **2016**, *7*, 1862-1866
B**TPE**AQ-cRGD dots	White light irradiation	100 mW cm^{-2}	0.38	*ACS Appl. Mater. Interfaces*, **2016**, *8*, 21193-21200
cRGD-siVEGF-TTD	White light irradiation	200 mW cm^{-2}	0.68	*Chem. Commun.,* **2016**, *52*, 2752-2755
TfR/**TPE**TH-2T7	White light irradiation	100 mW cm^{-2}	0.92	*Anal. Chem.*, **2016**, *88*, 4841-4848
P**TPE**AQ-NP	White light irradiation	60 mW cm^{-2}	0.82	*Macromolecules*, **2016**, *49*, 5017-5025
TPETF-NQ-cRGD	White light irradiation	100 mW cm^{-2}	0.33	*J. Mater. Chem. B*, **2016**, *4*, 169-176
TPE-IQ-2O	White light irradiation	5W	-	*Chem. Sci.,* **2017**,*8,* 1822-1830
TPE-Py-FFGYSA	White light irradiation	100 mW cm^{-2}	-	*Chem. Sci.,* **2017***, 8,* 2191-2198
T-TTD dot	532 nm laser power	250 mW cm^{-2}	0.51	*ACS Nano*, **2017,** *11,* 3922−3932

3. DLS and SEM studies of PAIE-TPP NPs and PAIE NPs in the DMSO/water mixtures

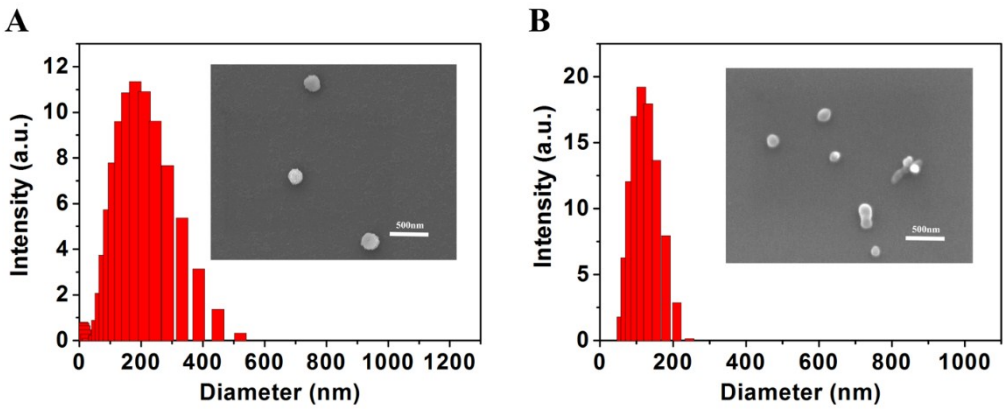

Figure S1. Particle size distribution and SEM image (inset) of the A) PAIE-TPP NPs and B) PAIE NPs in the DMSO/water (*v*/*v* = 2/98) mixtures (scale bar is 500 nm)

4. Average hydrodynamic diameter changes of AIE NPs in water and DMEM medium

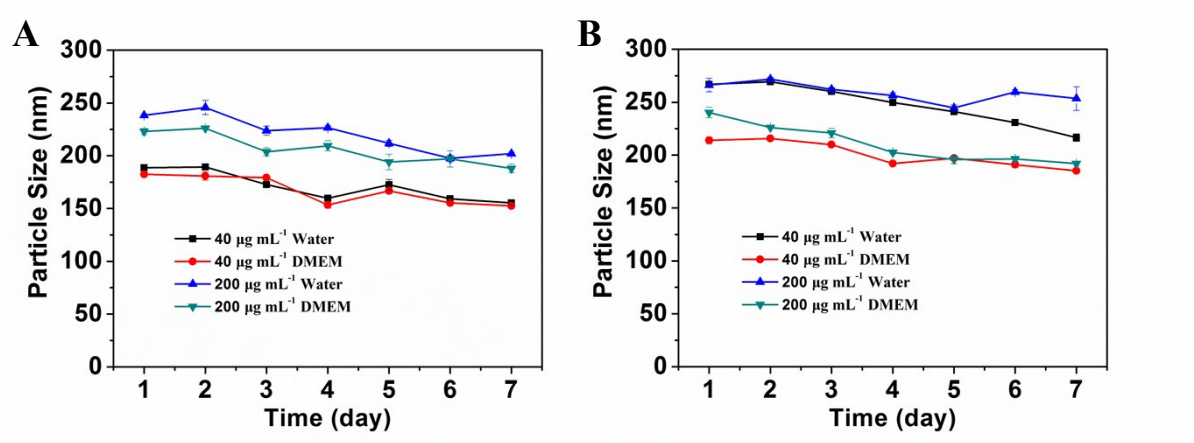

Figure S2. Average hydrodynamic diameter changes of A) PAIE NPs and B) PAIE-TPP NPs (40, 200 μg mL^{-1}) upon incubation in water and DMEM medium at 37 °C for 7 days.

5. Absorption and FL spectra of PAIE-TPP NPs and PAIE NPs in the THF/water mixtures

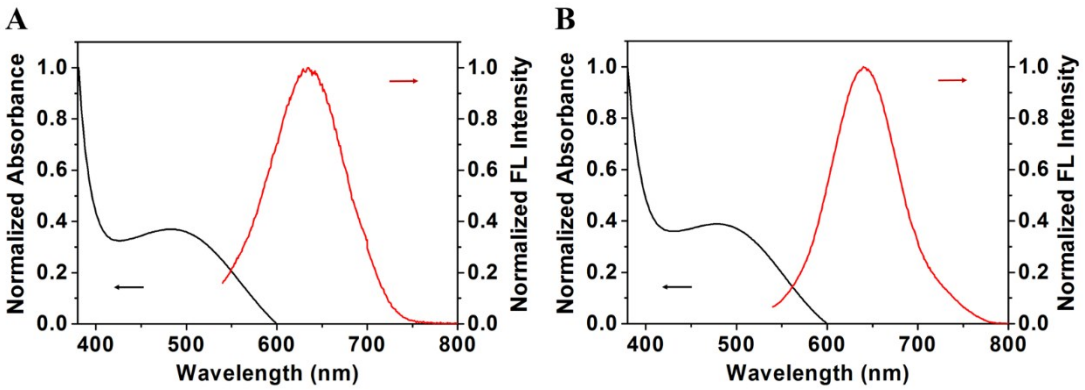

Figure S3. Normalized UV-vis absorbance and FL spectra of A) PAIE and B) PAIE-TPP in DMSO/water mixture (*v*/*v* = 2/98).

6. The ROS production of AIEM in solution

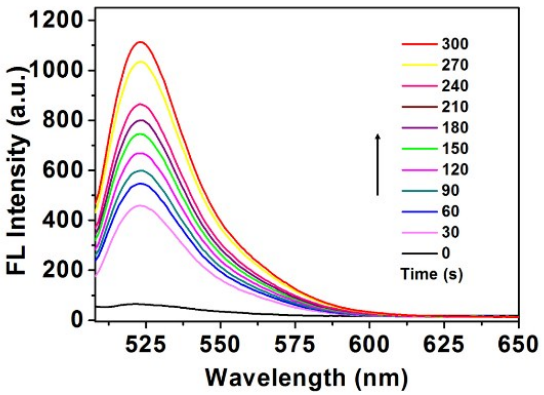

Figure S4. FL spectra of AIEM (25 μM) and DCF-DA (40 nM) mixture in water with different white light irradiation time (4 mW cm^{-2}).

7. Vitamin C inhibited the production of ROS in solution

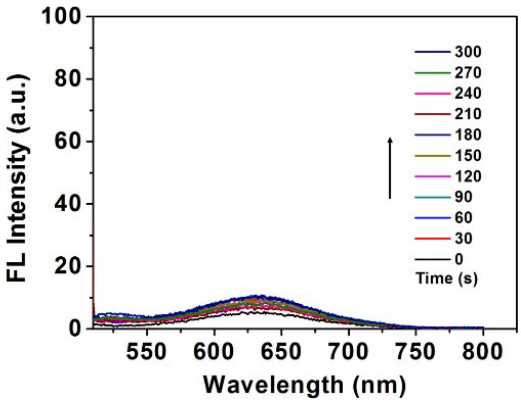

Figure S5. FL spectra of PAIE-TPP NPs (200 μg mL^{-1}) and DCF-DA (40 nM) mixture in water with Vitamin C (1mg mL^{-1}) added after different white light irradiation time (4 mW cm^{-2}).

8. Absorption spectra of ABDA mixed with RB and the decomposition rates

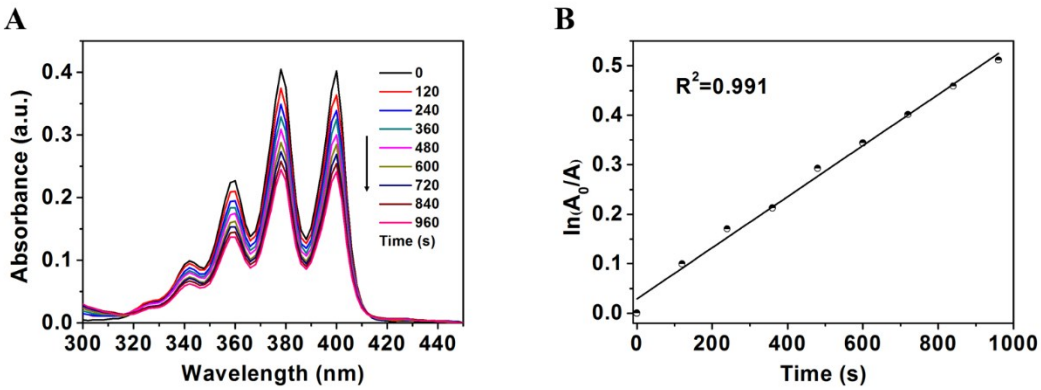

Figure S6. A) UV-vis absorbance changes of ROS indicator ABDA (200 μM) mixed with RB (5 μM) for different time duration of light irradiation (4 mW cm^{-2}). B) The decomposition rates of ABDA in the presence of RB.

9. Absorption spectra of PAIE-TPP NPs after different times of light irradiation

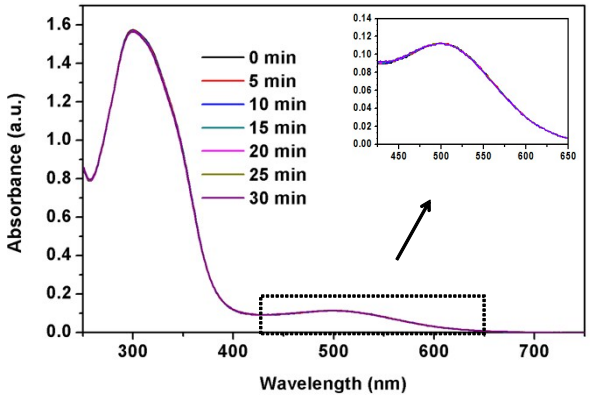

Figure S7. A) UV-vis absorbance spectra of PAIE-TPP NPs (100 μg mL^{-1}) after different times of light irradiation (10 mW cm^{-2}).

10. CLMS images of A549 cells after incubation with Mito-Tracker Green and PAIE-TPP NPs

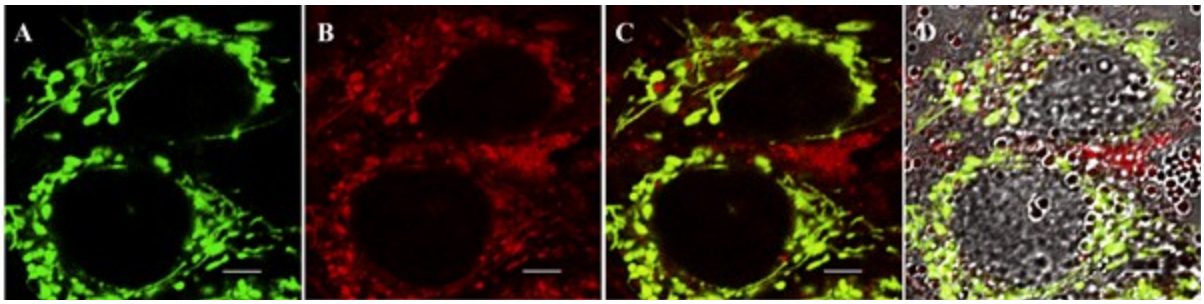

Figure S8. CLMS images of A549 cells after incubation with Mito-Tracker Green (50 nM) and PAIE-TPP NPs (40 μg mL^{-1}). A) Mito-Tracker Green channel. B) PAIE-TPP NPs channel. C) merge channel. D) bright-field images. AIE NPs, λ_{ex} = 488 nm, λ_{em} = 662-737 nm. Mito-Tracker Green, λ_{ex} = 488 nm, λ_{em} = 505-525 nm. The scale bar is 5 μm.

11. Flow cytometry of AIE NPs by A549 cells and HeLa cells

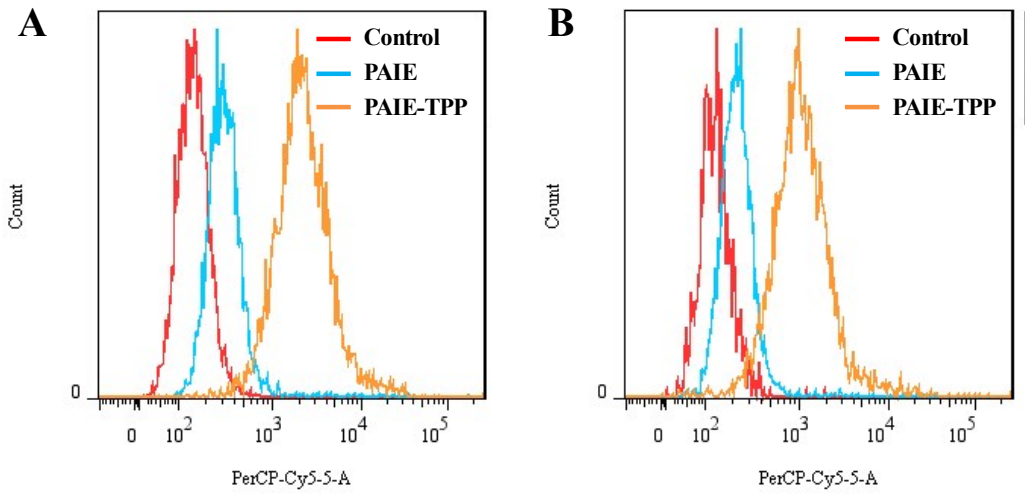

Figure S9. Flow cytometry of AIE NPs (PAIE-TPP or PAIE, 40 μg mL^{-1}) by A) A549 cells and B) HeLa cells.

12. *In vitro* imaging study of PAIE-TPP NPs in HeLa cells

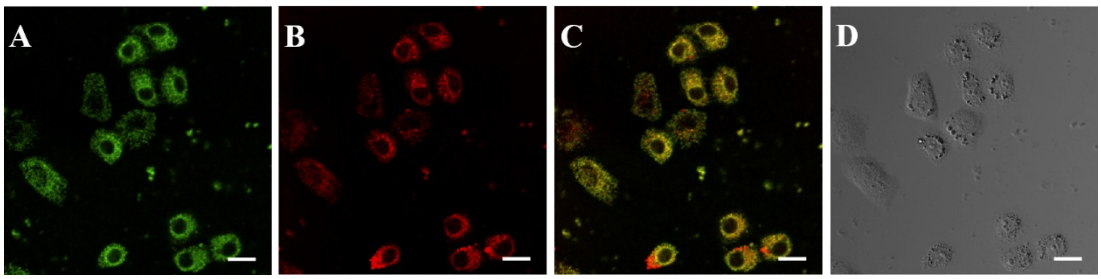

Figure S10. CLMS images of HeLa cancer cells after incubation with Mito-Tracker Green (50 nM) and AIE NPs (PAIE-TPP or PAIE, 40 μg mL^{-1}). A) Mito-Tracker Green channel, B) PAIE TPP channel, C) merge channel, D) bright-field images. PAIE-TPP, λ_{ex} = 488 nm λ_{em} = 662-737 nm. Mito-Tracker Green, λ_{ex} = 488 nm, λ_{em} = 505-525 nm. The scale bar is 20 μm.

13. Vitamin C inhibited the production of ROS in A549 cells

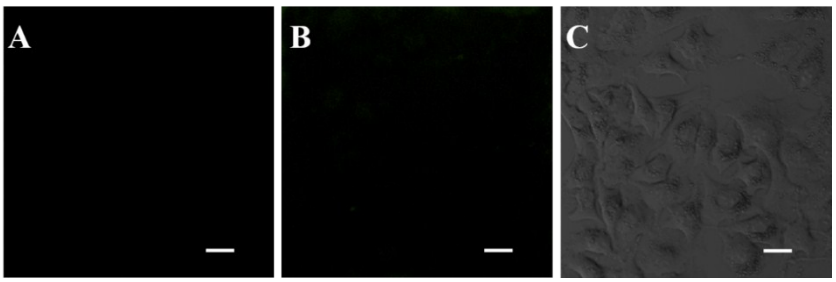

Figure S11. CLMS images of A549 cells after incubation with PAIE-TPP (40 μg mL^{-1}) and DCF-DA (10 μM) for white light irradiation A) 0 min, B) 8 min, C) bright-field images in the presence of ROS scavenger (Vitamin C, 1mg mL^{-1}). λ_{ex} = 488 nm, λ_{em} = 505-525 nm. The scale bar is 20 μm.

14. Intracellular ROS generation of PAIE NPs in A549 cells

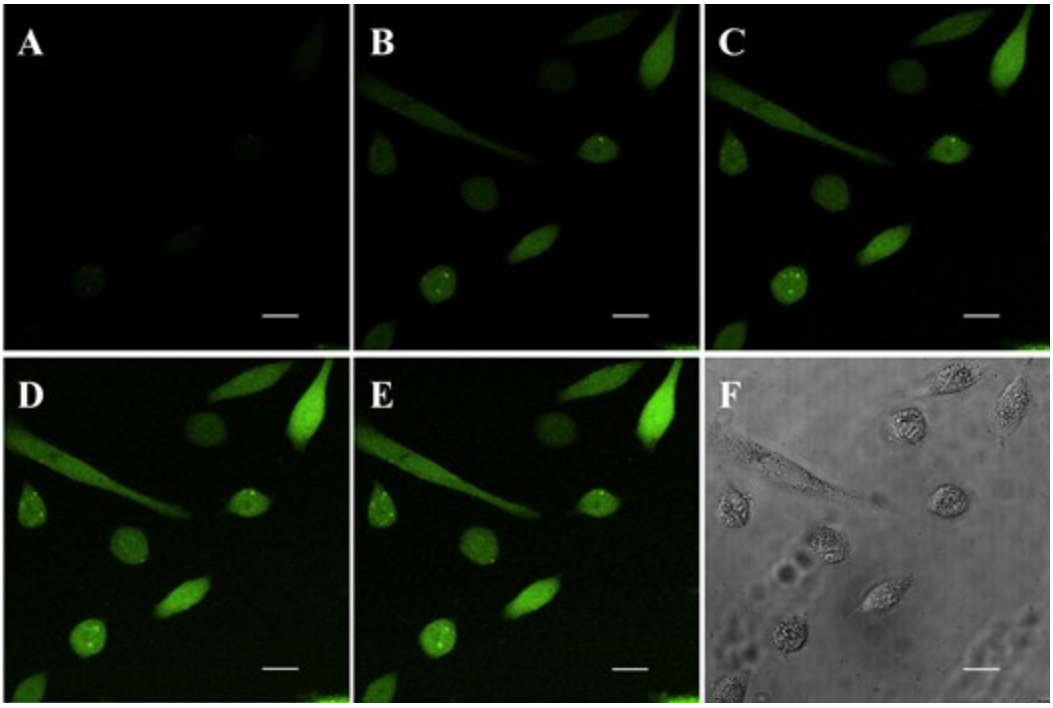

Figure S12. CLMS images of A549 cancer cells after incubation with PAIE NPs (40 μg mL^{-1}) and DCF-DA (10 μM) under white light irradiation for A) 0 min, B) 2 min, C) 4 min, D) 6 min, E) 8 min. F) is bright-field image. λ_{ex} = 488 nm, λ_{em} = 505-525 nm. The scale bar is 20 μm.

15. Cell viability of A549 cells and HeLa cells with PAIE

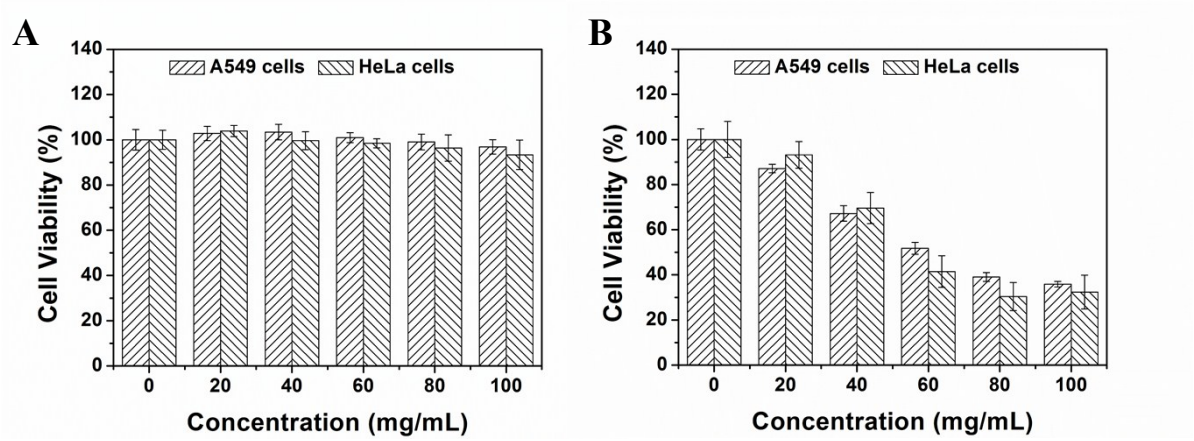

Figure S13. Cell viability of A549 cells and HeLa cells after incubation with different concentrations of PAIE NPs for 48 h A) in dark and B) under white light irradiation (10 mW cm^{-2}, 30 min per 12 h).

16. Cell viability of A549 cells and HeLa cells in dark and under light irradiation

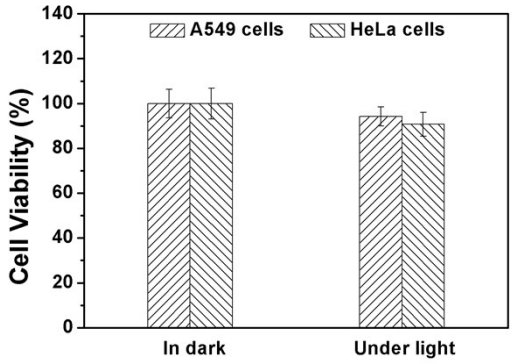

Figure S14. Cell viability of A549 cells and HeLa cells without NPs in dark and under light irradiation for 48 h (10 mW cm^{-2}, 30 min per 12 h).

17. Characterization of compounds

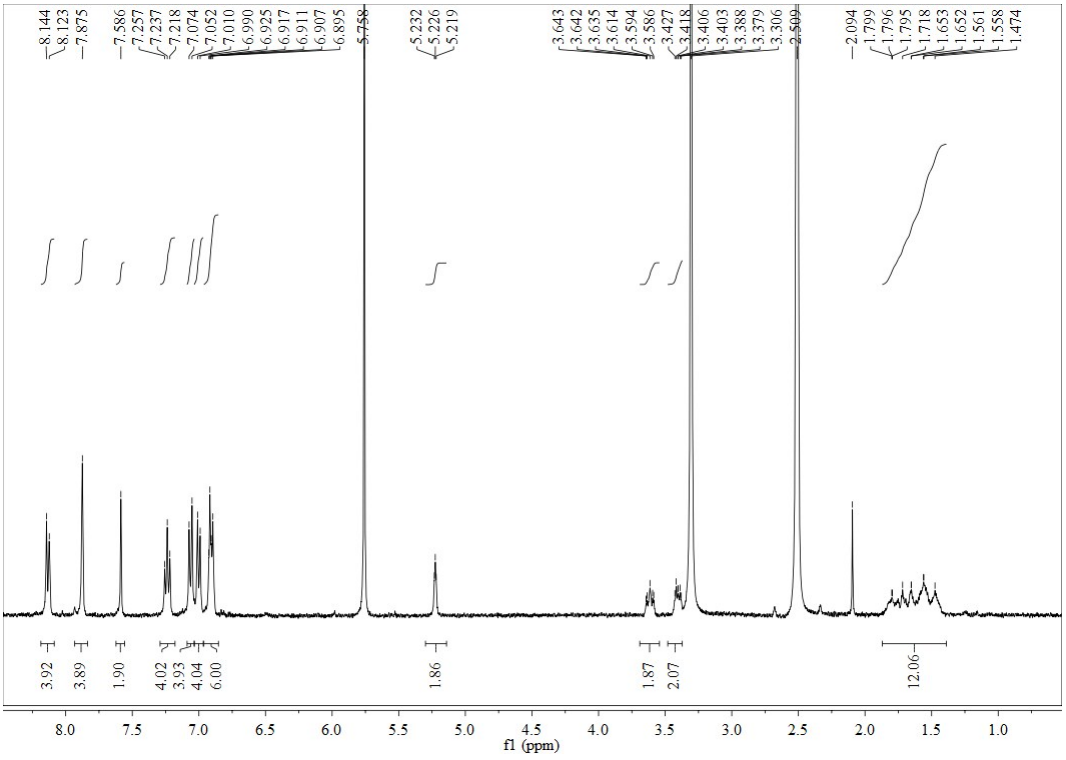

Figure S15. ^{1}H NMR spectrum of compound **3** in DMSO.

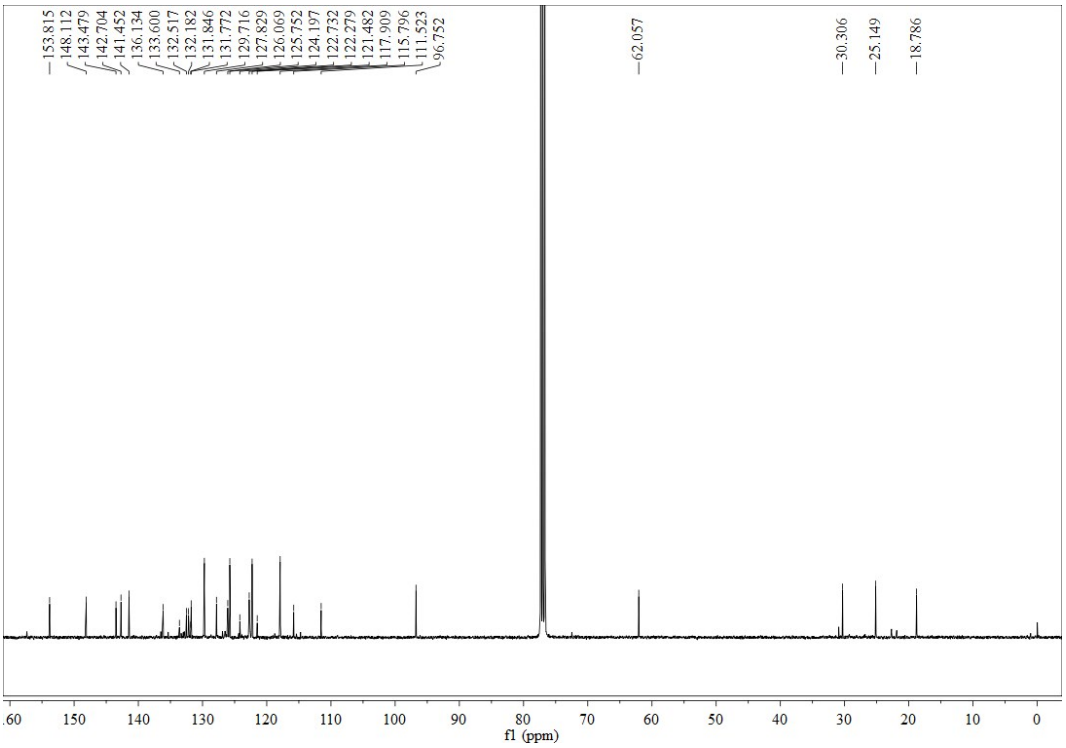

Figure S16. ^{13}C NMR spectrum of compound **3** in $CDCl_3$.

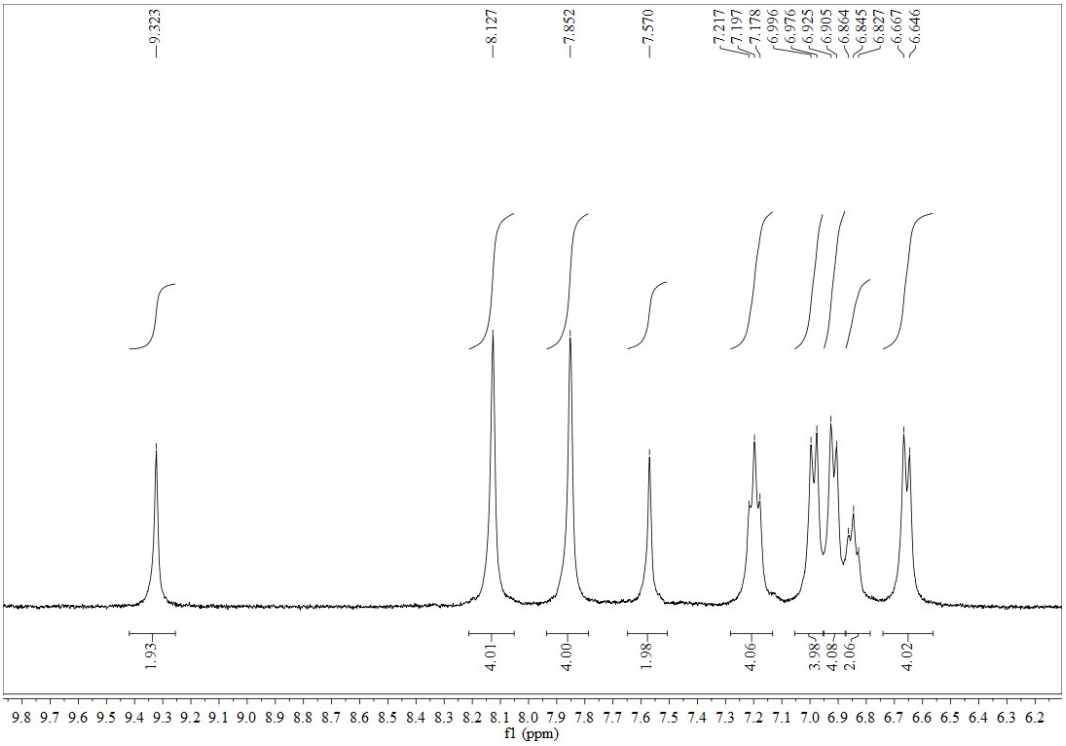

Figure S17. [1]H NMR spectrum of compound **4** in DMSO.

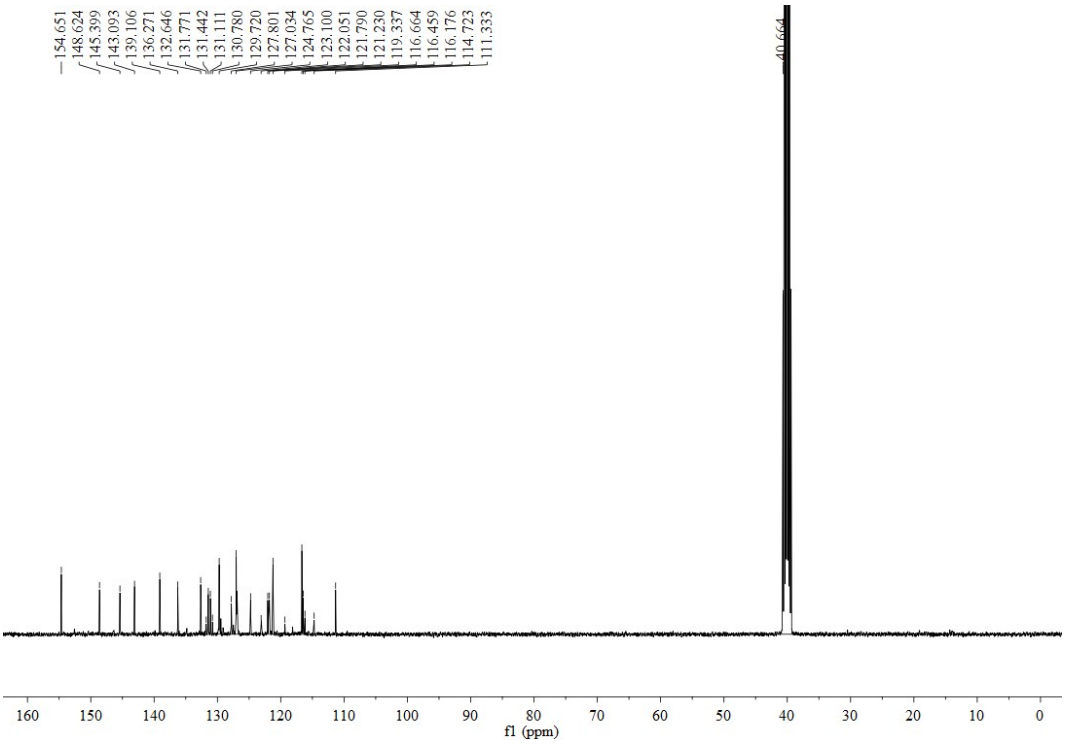

Figure S18. [13]C NMR spectrum of compound **4** in DMSO.

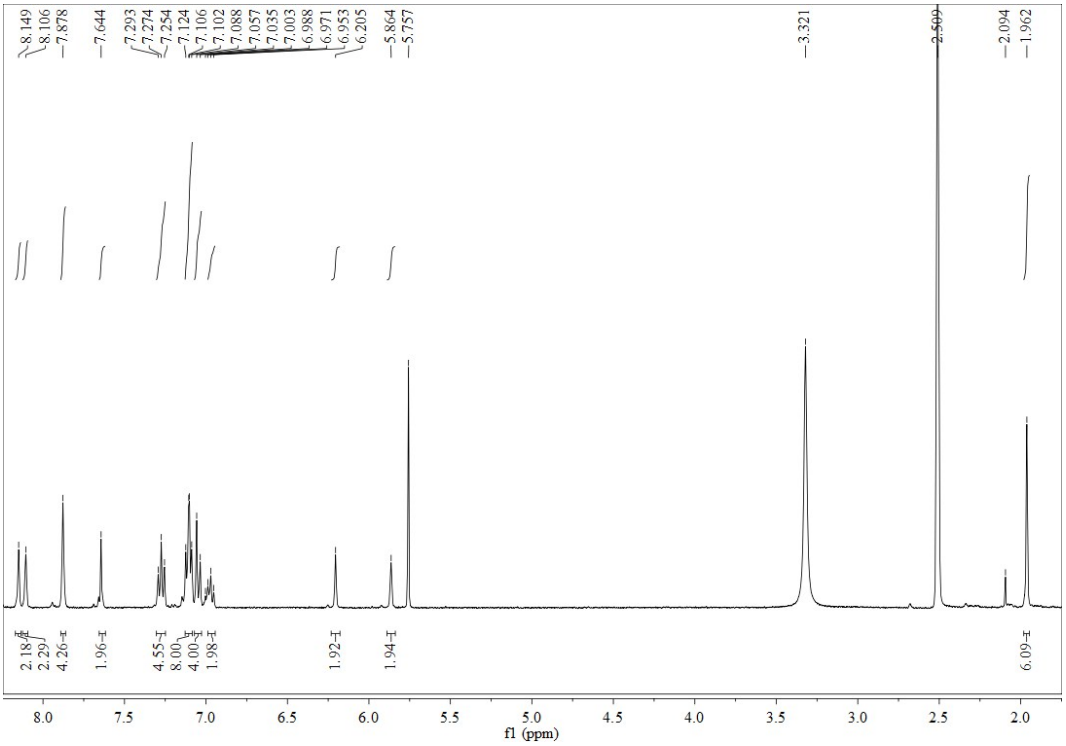

Figure S19. ^{1}H NMR spectrum of compound **5** in DMSO.

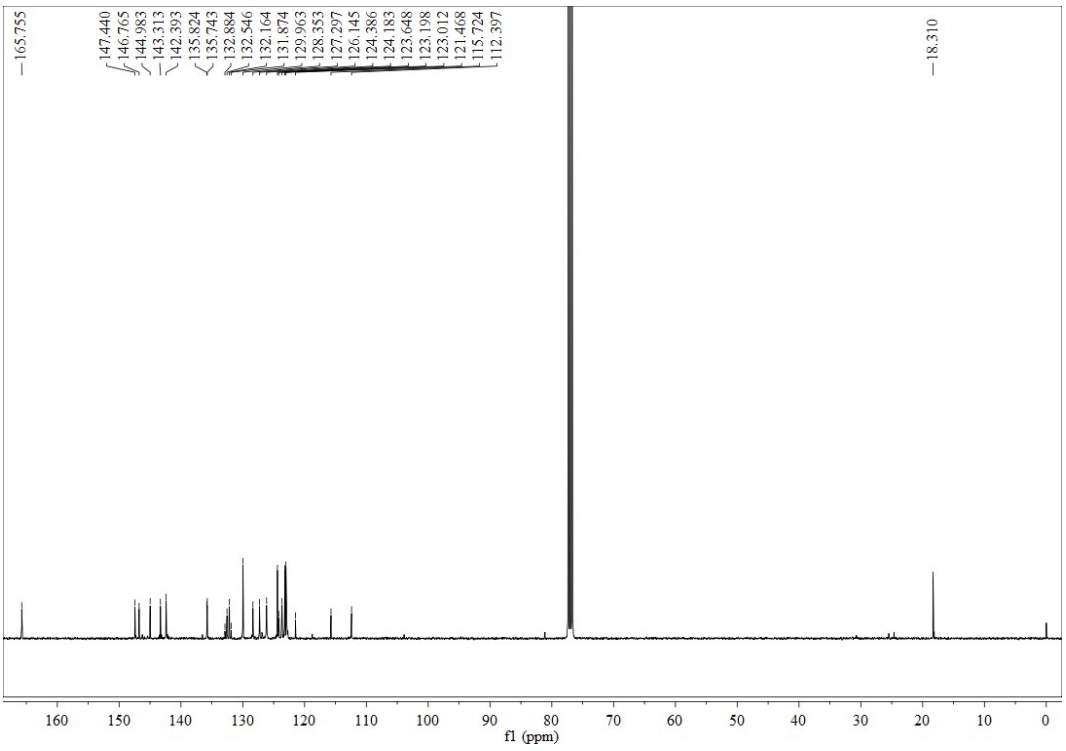

Figure S20. ^{13}C NMR spectrum of compound **5** in $CDCl_3$.

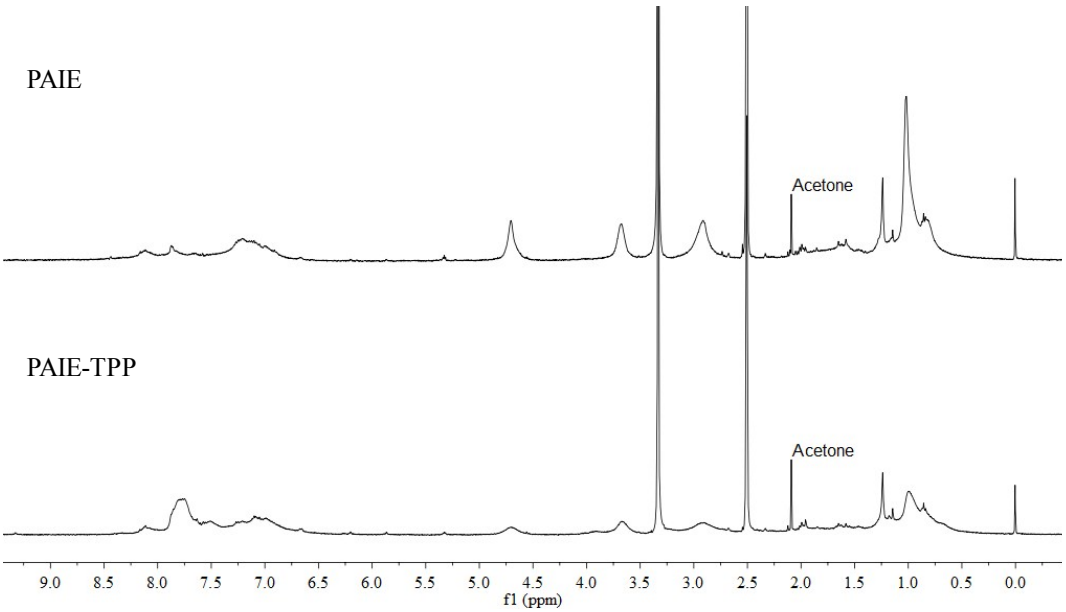

Figure S21. ^{1}H NMR spectra of polymer **PAIE** and **PAIE-TPP** in DMSO.

18. References

1 Z. Xie, B. Yang, L. Liu, M. Li, D. Lin, Y. Ma, G. Cheng, S. Liu. *J. Phys. Org. Chem.* 2005, **18**, 962.

2 K. M. Solntsev, P. L. McGrier, C. J. Fahrni, L. M. Tolbert, U. H. F. Bunz, *Org. Lett.* 2008, **10**, 2429.

3 H. Lu, Y. Zheng, X. Zhao, L. Wang, S. Ma, X. Han, B. Xu, W. Tian, H. Gao, *Angew. Chem. Int. Ed.* 2016, **55**, 155.

4 J. Strohalm, J. Kopeček, *Die Angewandte Makromolekulare Chemie* 1978, **70**, 109–118.

5 P. J. Stephens, F. J. Devlin, C. F. Chabalowski, M. J. Frisch, *J. Phys. Chem.* 1994, **98**, 11623.

6 P. C. Hariharan, J. A. Pople, *Chem. Acc.* 1973, **28**, 213.